Supplement of Atmos. Chem. Phys., 19, 617–638, 2019
https://doi.org/10.5194/acp-19-617-2019-supplement

Atmospheric Chemistry and Physics
Open Access

Supplement of

Characterization of VOCs and their related atmospheric processes in a central Chinese city during severe ozone pollution periods

Bowei Li et al.

Correspondence to: Steven Sai Hang Ho (stevenho@hkpsrl.org) and Sunling Gong (gongsl@cma.gov.cn)

1. Quality control and quality assurance (QC/QA)

In order to alleviate contamination from previous samples, canisters had to be repeatedly cleaned using humidified zero air before sampling. In order to inspect the cleanliness and vacuum in canisters, the pre-cleaned canisters, after storing for 24 h, were analyzed using GC-MS according to the same analytical procedures used to analyze the field samples. The canisters without any contamination were used for sampling. No obvious disturbances due to improperly activities (such as smoking, spray fumes, etc.) of sample collectors were present during the sampling events. Daily calibration of the GC-MSD/FID was performed using 2 ppbv standard mixtures to ensure the consistency and sensitivity of the system. The deviation in standard values was within ±20%. Abnormal QC/QA data with extremely high or low responses was recalibrated until the deviation was within the acceptable range.

2. PMF model

In brief, PMF is a diagnostic method involving multivariate analysis, and involves decomposing the integrated sample data (VOCs in this study) into two matrices, namely the source profiles and the source contributions (Jaars et al., 2018). The method takes advantage of other observation data, such as wind direction and speed. Detailed information on the application of PMF can be referred to the publications cited above and to the PMF 5.0 user manual (U.S. EPA, 2014).

Based on the chemical mass balance between the input concentrations of VOCs and the chemical profiles, PMF regarded the ambient data x_{ij}, namely the concentration of j^{th} constituent in i^{th} sample, as the gross values contributed by p sources according to Eq. (1).

$$X_{ij} = \sum_{k=1}^{p} g_{ik} f_{kj} + e_{ij} \qquad (1)$$

where g_{ik} stands for the contribution of k^{th} factor in the i^{th} sample, while f_{kj} is the load of j^{th} compound in the k^{th} source and the e_{ij} is the relevant residual.

In order to avoid negative source contributions, a penalty function was adopted for constraints. Each data point can be individually weighed in the model, while the samples with lots of missing values were excluded.

Based on the algorithm for uncertainties (U), expressed as Q values, the stability of running results was assessed according to Eq. (2).

$$Q = \sum_{i=1}^{n}\sum_{j=1}^{m}\left[\frac{x_{ij} - \sum_{k=1}^{p} g_{ik} f_{kj}}{u_{ij}}\right]^2 \qquad (2)$$

where u_{ij} stands for the uncertainty of the j^{th} compound in i^{th} sample.

In the PMF model, uncertainty is a function to evaluate the deviations in sampling and analysis procedure (Paatero, 2007). The uncertainty (U) can be calculated based on Eq. (3) (Polissar et al., 1998).

$$U = \begin{cases} \sqrt{(EF \times concentration)^2 + (MDL)^2} & \text{(conc.>MDL)} \\ \frac{5}{6} MDL & \text{(conc} \leq \text{MDL)} \end{cases} \qquad (3)$$

where EF signifies the error fraction that equals 100 times of the percentage uncertainty.

3. Source identification

Source profiles showed that the sites had similar regional characteristic. There was a strong common source (factor 1) for C_2 - C_5 n-alkanes and certain amounts of C_2 - C_4 alkenes, benzene, toluene, acetylene and NO_2. It is reported that i-pentane and aromatics (such as, benzene, toluene, ethylbenzene and m/p-xylene) are usually originated from gasoline evaporation (Watson et al., 2001), while isobutane and n-butane are emitted from vehicles fueled with LPG/CNG (Li et al., 2017;Liu et al., 2008), in addition, the ratio of toluene close to 2 is defined as vehicle emission.

The second factor was characterized based upon significant loading of toluene, ethylbenzene, m/p-xylene, o-xylene and m-ethyltoluene. According to previous studies (Yuan et al., 2010;Wang et al., 2014), toluene and C_8 - C_9 aromatics were the major VOCs emitted from paint applications. Therefore, factor 2 was assigned as the solvent use. This is consistent with the real situation that there were widespread road paving and building constructions in Zhengzhou. In addition, car decoration, printing, and furniture manufacturing, which are associated with the use of adhesives, were also included in this source category.

Factor 3 was dominated by c/t-2-butene, 1-butene and c/t-2-pentene. According to our unpublished data, these species were abundant in ambient air next to oil gas stations. This factor was thus categorized as the oil evaporation. The profile at MEM was contained more C_8-C_{10} alkanes and m-ethyltoluene, which were abundant in diesel vapor, indicating the heavier diesel evaporation at this site.

The fourth factor shows a dominant loading of cyclohexane, styrene, 2-methylhexane, 3-methylhexane and 2,3-dimethylpentane. The first three VOCs were identified as the components heavily impacted by petrochemical industries (Jobson et al., 2004). Therefore, this source was defined as the petrochemical.

Factor 5 was composed of acetylene, ethylene, propylene, benzene, ethane, propane and several amounts of C_7-C_{10} alkanes. Both coal and biomass burning could produce large amounts of acetylene (Ho et al., 2009), benzene, ethylene and propylene. According to lower level of toluene in this factor, this factor was referred to as the coal+biomass burning.

Factor 6 was distinguished by extremely high compositions of isoprene, a species mainly produced by vegetation through photosynthesis (Millet et al., 2016). Even though it can be emitted from traffic-related sources (Yuan et al., 2009), this can be possibly ignored by its poor correlations with other source makers of vehicle exhaust (e.g., i-pentane and ethylene). Therefore, this factor was identified as the biogenic emissions.

Table S1. Detailed information of monitoring equipment for SO_2, CO, NO_x, O_3 and meteorological factors

Targets	Equipment	Model
SO_2	Pulsed Fluorescence SO_2 Analyzer	Model 43i, Thermo, Inc.
CO	Gas Filter Correlation CO Analyzer	Model 48i, Thermo, Inc.
NO-NO_2-NOx	Chemiluminescence NO-NO_2-NOx Analyzer	Model 42i, Thermo, Inc.
O_3	ultra-violet (UV) photometric O_3 analyzer	Model 49i, Thermo, Inc.
Meteorological data	multi-parameter automatic weather station	Milos 520, Vaisala, Inc.

Table S2. Detailed information on the calibration curve for 57VOCs and their MIR

	NO.	**Species**	**R^2**	**MDL (pptv)**	**RSD**	**MIR**		**NO.**	**Species**	**R^2**	**MDL (pptv)**	**RSD**	**MIR**
Alkane	1	Ethane	0.9998	6.8	5%	0.28	**Alkene**	29	Ethylene	0.9997	12.5	10%	9
	2	Propane	0.9998	2.8	2%	0.49		30	Propylene	0.9998	6.2	5%	11.66
	3	Isobutane	0.9998	3.2	3%	1.23		31	Trans-2-butene	1	3.6	6%	15.16
	4	n-Butane	0.9998	6.7	5%	1.15		32	1-Butene	0.9995	7.8	6%	9.73
	5	Cyclopentane	0.9971	8.5	7%	0.09		33	Cis-2-butene	0.9997	6.8	6%	14.24
	6	Isopentane	0.9999	5.5	4%	0.93		34	1,3-butadiene	0.9874	13.5	8%	
	7	n-Pentane	0.9999	6.6	5%	0.88		35	1-Pentene	0.9764	6.3	5%	7.21
	8	2,2-Dimethyl-butane	0.9963	5.4	4%	1.17		36	Trans-2-pentene	0.9964	10.1	7%	10.56
	9	2,3-Dimethylbutane	0.9966	7.6	6%	0.97		37	Isoprene	0.9966	7.7	6%	10.61
	10	2-Methylpentane	0.9958	8	6%	1.5		38	Cis-2-pentene	0.9965	8.6	7%	10.38
	11	3-Methylpentane	0.9967	5.4	4%	1.8		39	1-Hexene	0.9961	11.4	9%	4.4
	12	n-Hexane	0.9967	7.3	6%	1.24	**Alkyne**	40	Acetylene	0.9996	7.1	5%	0.95
	13	2,4-Dimethylpentane	0.9972	9.6	7%	1.55	**Aromatic**	41	Benzene	0.9975	6.5	5%	0.72
	14	Methyl-cyclopentane	0.9974	5.8	5%	2.19		42	Toluene	0.9963	4.3	4%	4
	15	2-Methyl-hexane	0.9968	8.6	7%	1.19		43	Ethyl-benzene	0.9955	4.8	4%	3.04
	16	Cyclohexane	0.9958	7.7	6%	1.25		44	m,p-Xylene[a]	0.9969	12.5	5%	7.8
	17	2,3-Dimethyl-pentane	0.9969	6.2	5%	1.34		45	o-Xylene	0.9954	5.2	4%	7.64
	18	3-Methyl-hexane	0.9946	8.8	7%	1.61		46	Styrene	0.9961	10.6	8%	1.73
	19	2,2,4-Trimethylpentane	0.9975	7.1	6%	1.26		47	Isopropylbenzene	0.9947	4.3	4%	2.52
	20	n-Heptane	0.9974	9	7%	1.07		48	n-Propylbenzene	0.9929	1.6	1%	2.03
	21	Methyl-cyclohexane	0.9972	5.8	5%	1.7		49	m-Ethyltoluene	0.991	7.3	6%	7.39
	22	2,3,4-Trimethylpentane	0.9976	5.7	5%	1.03		50	p-Ethyltoluene	0.9994	8.4	7%	4.44
	23	2-Methyl-heptane	0.9971	7	6%	1.07		51	1,3,5-Trimethyl-benzene	0.9994	6.1	5%	11.76
	24	3-Methyl-heptane	0.9974	6.7	5%	1.24		52	o-Ethyltoluene	0.9995	4.3	4%	5.59
	25	n-Octane	0.9973	7.6	6%	0.9		53	1,2,4-Trimethyl-benzene	0.9983	9.7	8%	8.87
	26	n-Nonane	0.9963	3.4	3%	0.78		54	1,2,3-Trimethyl-benzene	0.9927	9.7	8%	11.97
	27	n-Decane	0.9935	7.8	6%	0.68		55	m-Diethylbenzene	0.9967	5.2	4%	7.1
	28	n-Undecane	0.9919	7.5	6%	0.61		56	p-Diethylbenzene	0.995	4.2	3%	4.43

[a] *m*-Xylene and *p*-Xylene are co-eluted in the chromatographic separation.

Table S3. The correlation coefficient (R^2) between observed and predicted values for each compound at the four sites

species	JK	MEM	YH	GS
ethane	0.73	0.59	0.87	0.68
propane	0.82	0.89	0.87	0.45
isobutane	0.97	0.87	0.64	0.93
n-butane	0.73	0.93	0.93	0.66
isopentane	0.66	0.40	0.81	0.76
n-pentane	0.84	0.65	0.63	0.86
methyl-cyclopentane	0.98	0.86	0.77	0.89
2-methyl-hexane	0.99	0.97	0.85	0.98
cyclohexane	1.00	0.95	0.92	0.95
2,3-dimethyl-pentane	0.99	0.99	0.97	0.99
3-methyl-hexane	0.99	0.97	0.88	0.99
2,2,4-trimethyl-pentane	0.77	0.89	0.81	0.80
n-heptane	0.99	0.87	0.96	0.77
n-octane	0.77	0.88	0.61	0.72
n-decane	0.52	0.73	0.15	0.70
ethylene	0.83	0.92	0.33	0.91
propylene	0.85	0.88	0.81	0.87
trans-2-butene	0.90	0.87	0.93	0.73
1-butene	0.93	0.95	0.94	0.74
cis-2-butene	0.93	0.96	0.97	0.80
trans-2-pentene	0.87	0.93	0.97	0.84
isoprene	0.98	0.90	0.90	0.88
cis-2-pentene	0.87	0.96	0.94	0.74
acetylene	0.43	0.80	0.73	0.82
benzene	0.96	0.79	0.39	0.91
toluene	0.94	0.85	0.86	0.52
ethyl-benzene	0.91	0.93	0.99	0.97
m,p-xylene[a]	0.88	0.99	0.97	0.88
o-xylene	0.94	0.99	0.97	0.88
styrene	0.74	0.82	0.66	0.87
m-ethyltoluene	0.74	0.93	0.94	0.81
NO_2	0.81	0.57	0.73	0.65

[a] *m*-Xylene and *p*-Xylene are co-eluted in the chromatographic separation.

Table S4 Error estimation summary results, i.e. BS mapping for the four sites

(a) JK

	biogenic	oil gas evaporation	petrochemical	vehicle emission	solvent usage	coal+biomass burning	Unmapped
Boot Factor 1	100	0	0	0	0	0	0
Boot Factor 2	0	100	0	0	0	0	0
Boot Factor 3	0	1	98	1	0	0	0
Boot Factor 4	0	0	0	100	0	0	0
Boot Factor 5	0	0	0	0	100	0	0
Boot Factor 6	0	0	0	3	0	97	0

(b) MEM

	vehicle emission	biogenic	petrochemical	solvent usage	coal+biomass burning	oil gas evaporation	Unmapped
Boot Factor 1	100	0	0	0	0	0	0
Boot Factor 2	0	100	0	0	0	0	0
Boot Factor 3	1	0	99	0	0	0	0
Boot Factor 4	0	0	0	100	0	0	0
Boot Factor 5	0	0	0	0	100	0	0
Boot Factor 6	0	0	0	0	0	100	0

(c) YH

	solvent usage	petrochemical	vehicle emission	coal+biomass burning	oil gas evaporation	biogenic	Unmapped
Boot Factor 1	99	0	1	0	0	0	0
Boot Factor 2	1	99	0	0	0	0	0
Boot Factor 3	0	2	94	2	2	0	0
Boot Factor 4	0	0	0	99	1	0	0
Boot Factor 5	0	0	0	1	99	0	0
Boot Factor 6	0	0	0	0	0	100	0

(d) GS

	petrochemical	biogenic	oil gas evaporation	coal+biomass burning	vehicle emission	solvent usage	Unmapped
Boot Factor 1	94	0	0	1	0	2	3
Boot Factor 2	0	100	0	0	0	0	0
Boot Factor 3	1	0	91	1	1	4	2
Boot Factor 4	0	0	0	100	0	0	0
Boot Factor 5	0	0	4	0	82	10	4
Boot Factor 6	0	0	0	0	0	100	0

Table S5. The ratio of Q/Q(exp) at factor size ranged from 3-9 at the four sites

	JK	MEM	YH	GS
3	2.62	2.12	2.43	2.73
4	2.07	1.62	1.96	2.19
5	1.56	1.23	1.57	1.86
6	1.27	1.01	1.23	1.69
7	1.15	0.80	1.10	1.40
8	1.03	0.71	1.01	1.24
9	0.94	0.66	0.92	1.18

Table S6. The average mixing ratios of SO_2, NO_x, CO and O_3 from May to September 2017

	SO_2(ppb)	**NOx(ppb)**	**CO(ppm)**	**O_3 (ppb)**
May	9.55	35.76	0.70	86.73
June	5.49	31.76	0.71	99.32
July	2.52	20.62	0.69	76.27
August	2.98	25.48	0.89	76.92
September	5.72	52.60	0.96	61.31

Table S7. Identified source categories by PMF and their corresponding markers

Source	**Source category**	**Markers**	**Reference**
1	vehicle emission	C2-C5 alkanes, NO_2	(Watson et al., 2001)
2	coal+biomass burning	ethane, ethylene, acetylene, benzene	(Liu et al., 2008;Zhang et al., 2013)
3	solvent usage	toluene, ethylbenzene, xylenes	(Yuan et al., 2010;Wang et al., 2014)
4	oil gas evaporation	C4-C5 alkenes, n-heptane	(Wang et al., 2017)
5	petrochemical	methyl-cyclopentane, cyclohexane, 3-Methyl-hexane, 2-Methyl-hexane, styrene	(Liu et al., 2008;Jobson et al., 2004)
6	biogenic	Isoprene	(Millet et al., 2016)

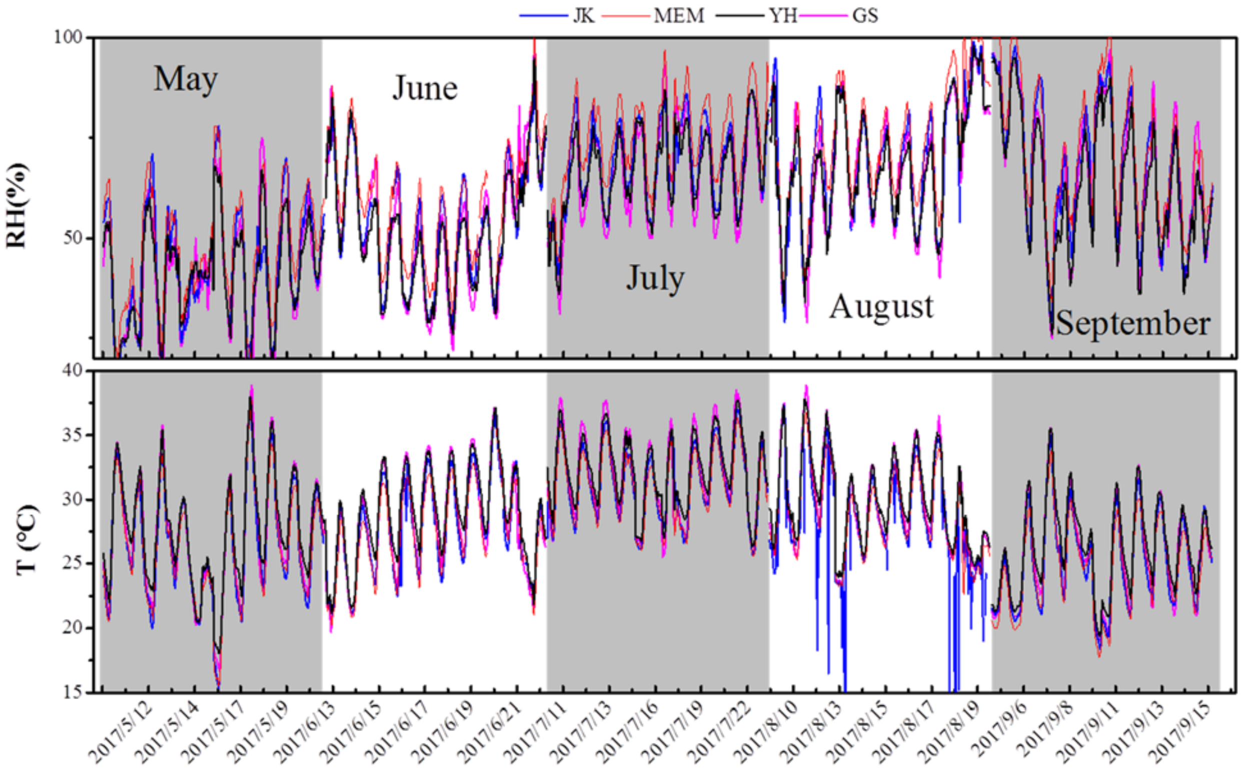

Fig. S1. The temperature and relative humidity at each site during sampling period

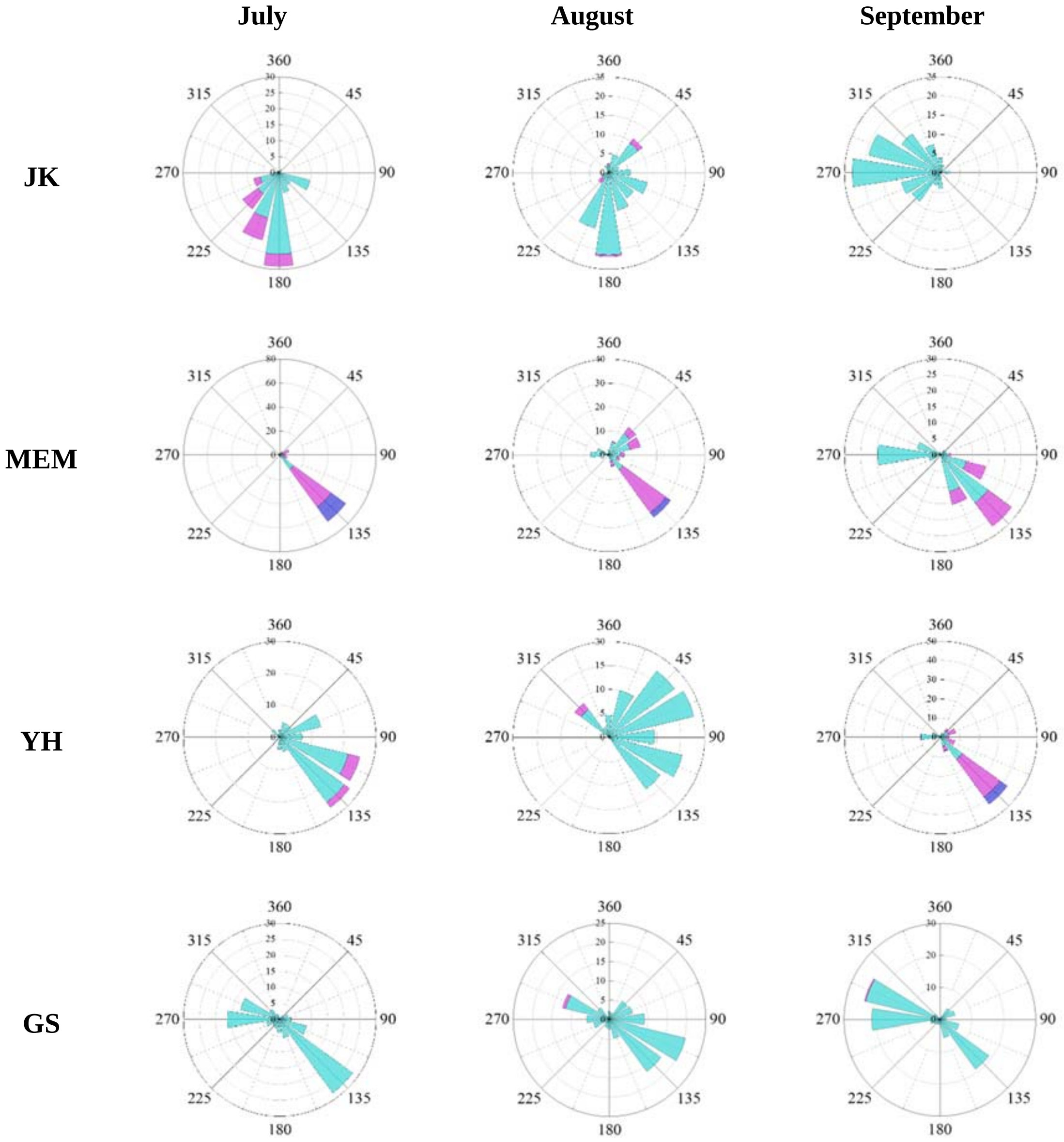

Fig. S2. The wind distribution at each site in July, August and September

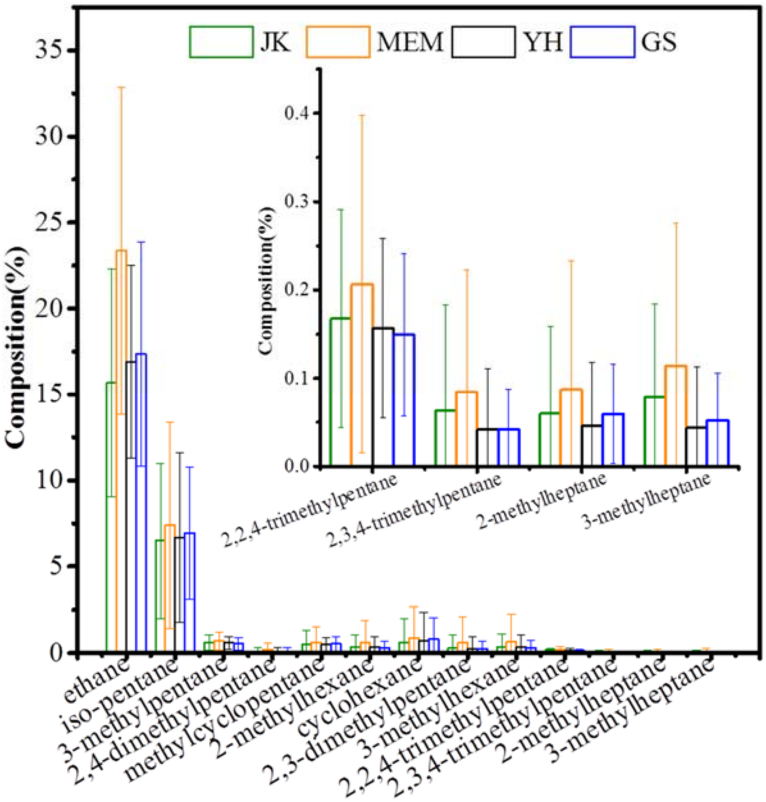

Fig. S3. Compositions of ethane, iso-pentane and C_7-C_8 alkanes at JK, MEM, YH and GS

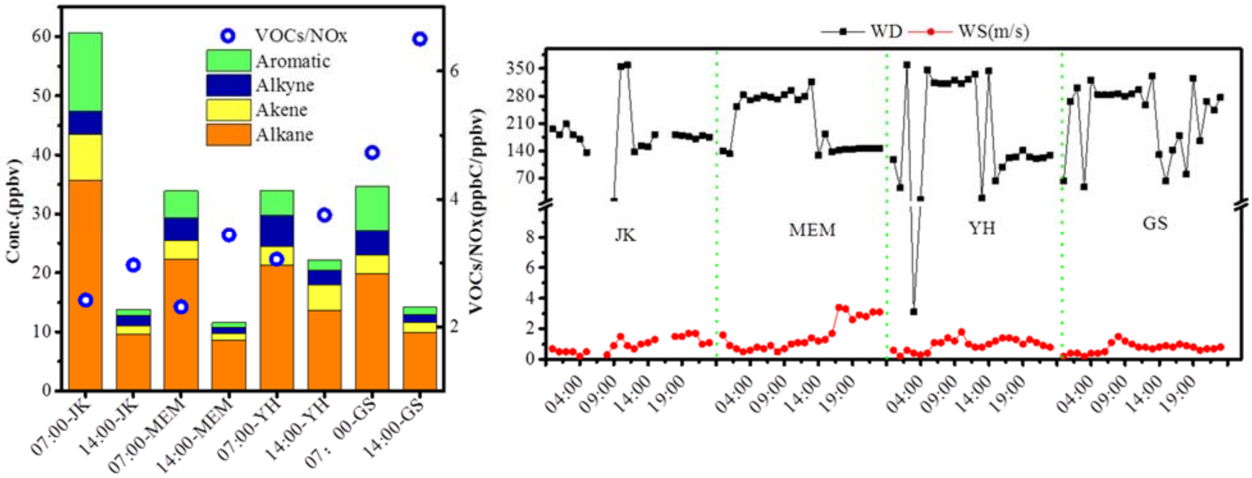

Fig.S4. Temporal variation of compositions, VOCs/NO$_x$, wind direction and wind speed on 10th of August 2017

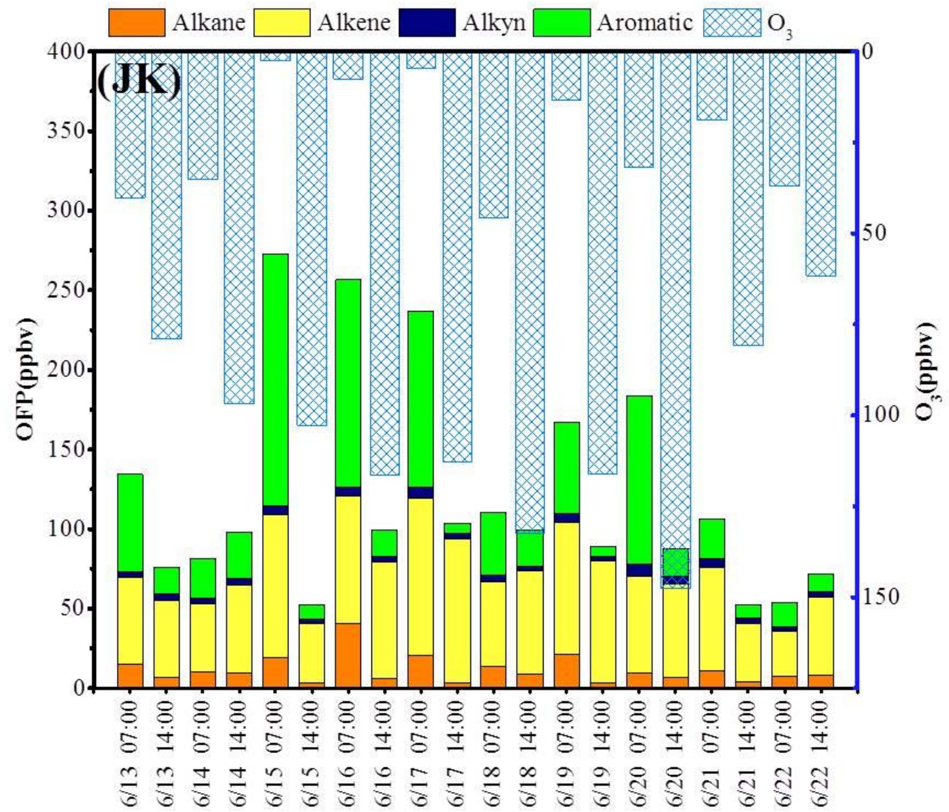
Alkane
Alkene
Alkyn
Aromatic
O3
(JK)
OFP(ppbv)
O_3(ppbv)
400
350
300
250
200
150
100
50
0
0
50
100
150
6/13 07:00
6/13 14:00
6/14 07:00
6/14 14:00
6/15 07:00
6/15 14:00
6/16 07:00
6/16 14:00
6/17 07:00
6/17 14:00
6/18 07:00
6/18 14:00
6/19 07:00
6/19 14:00
6/20 07:00
6/20 14:00
6/21 07:00
6/21 14:00
6/22 07:00
6/22 14:00

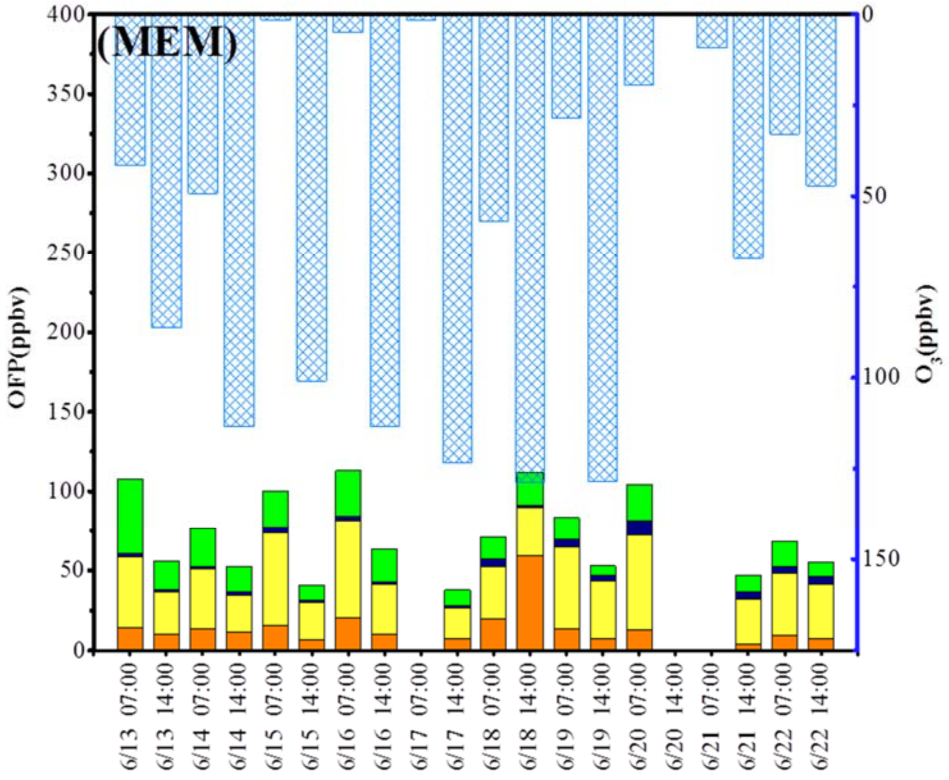
(MEM)
OFP(ppbv)
O_3(ppbv)
400
350
300
250
200
150
100
50
0
0
50
100
150
6/13 07:00
6/13 14:00
6/14 07:00
6/14 14:00
6/15 07:00
6/15 14:00
6/16 07:00
6/16 14:00
6/17 07:00
6/17 14:00
6/18 07:00
6/18 14:00
6/19 07:00
6/19 14:00
6/20 07:00
6/20 14:00
6/21 07:00
6/21 14:00
6/22 07:00
6/22 14:00

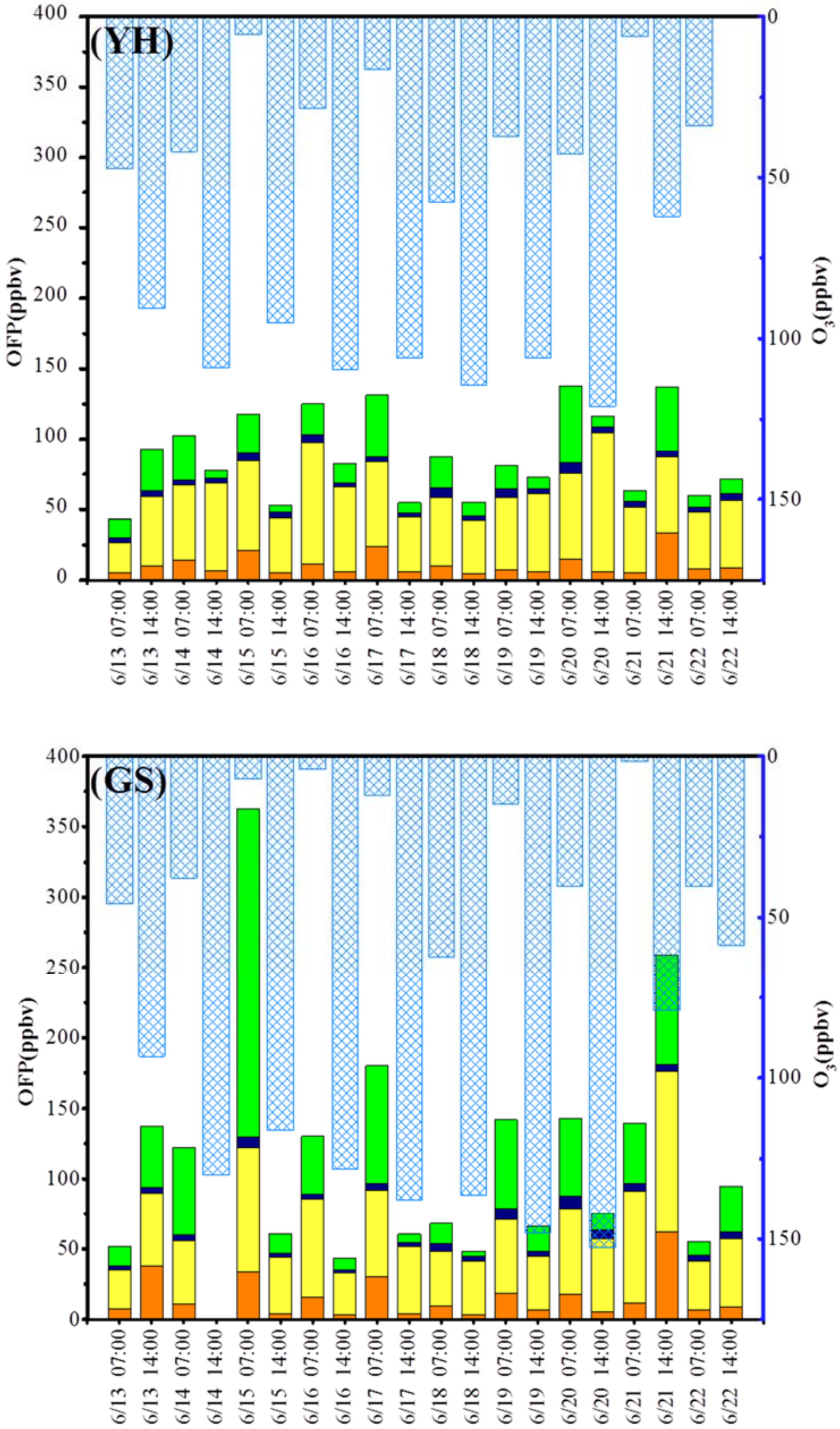

Fig.S5. Spatio-temporal variations in OFP of each organic group, and mixing ratios of O_3 in June.

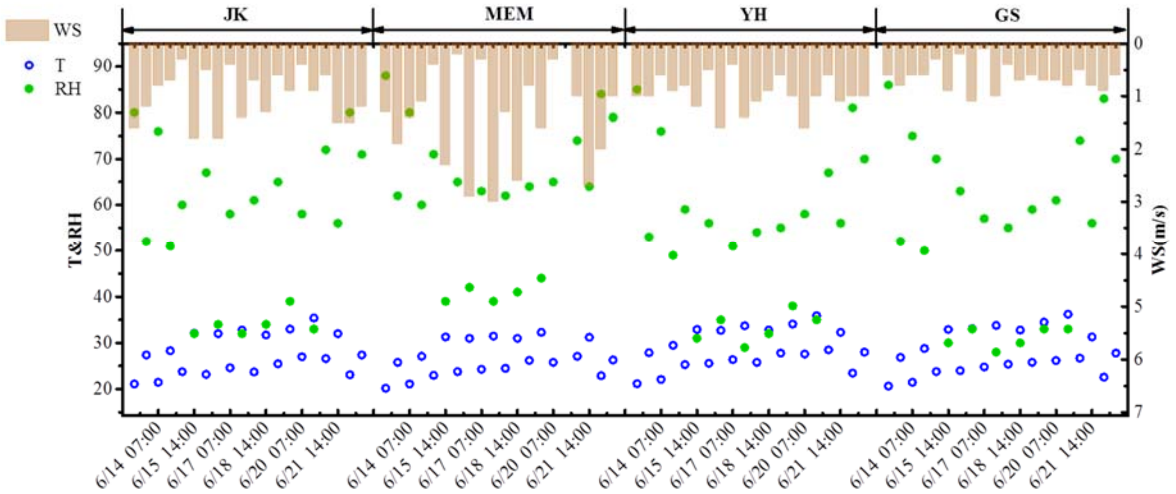

Fig.S6. Spatio-temporal variations in meterological factors in June

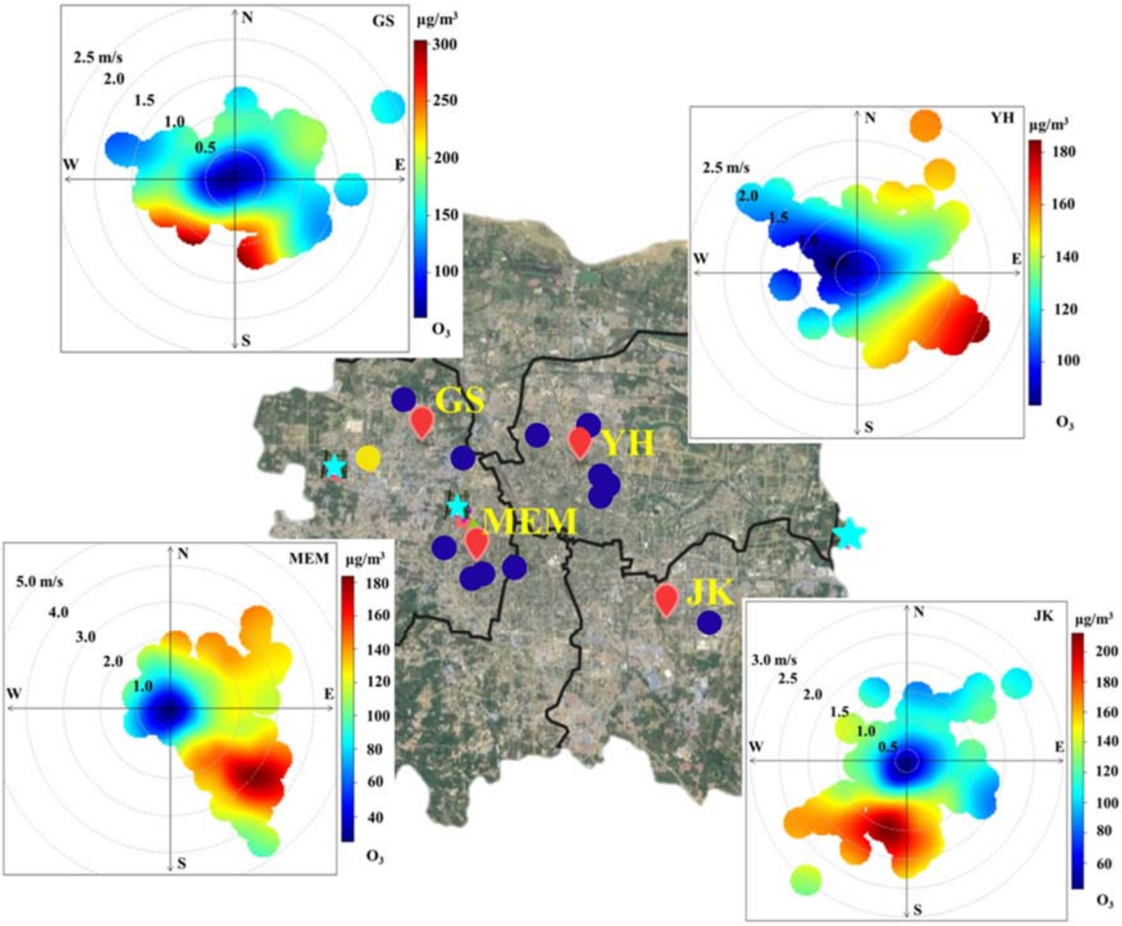

Fig. S7. Relationship among O_3 (μg m^{-3}), wind direction and wind speed (m s^{-1}) during sampling period in June, 2017

Reference

Ho, K. F., Lee, S. C., Ho, W. K., Blake, D. R., Cheng, Y., Li, Y. S., Ho, S. S. H., Fung, K., Louie, P. K. K., and Park, D.: Vehicular emission of volatile organic compounds (VOCs) from a tunnel study in Hong Kong, Atmos. Chem. Phys., 9, 7491–7504, 2009.

Jaars, K., Vestenius, M., van Zyl, P. G., Beukes, J. P., Hellén, H., Vakkari, V., Venter, M., Josipovic, M., and Hakola, H.: Receptor modelling and risk assessment of volatile organic compounds measured at a regional background site in South Africa, Atmos. Environ., 172, 133-148, https://doi.org/10.1016/j.atmosenv.2017.10.047, 2018.

Jobson, B. T., Berkowitz, C. M., Kuster, W. C., Goldan, P. D., Williams, E. J., Fesenfeld, F. C., Apel, E. C., Karl, T., Lonneman, W. A., and Riemer, D.: Hydrocarbon source signatures in Houston, Texas: Influence of the petrochemical industry, J. Geophys. Res., 109, D24305, https://doi.org/10.1029/2004jd004887, 2004.

Li, B., Ho, S. S. H., Xue, Y., Huang, Y., Wang, L., Cheng, Y., Dai, W., Zhong, H., Cao, J., and Lee, S.: Characterizations of volatile organic compounds (VOCs) from vehicular emissions at roadside environment: The first comprehensive study in Northwestern China, Atmos. Environ., 161, 1-12, https://doi.org/10.1016/j.atmosenv.2017.04.029, 2017.

Liu, Y., Shao, M., Fu, L., Lu, S., Zeng, L., and Tang, D.: Source profiles of volatile organic compounds (VOCs) measured in China: Part I, Atmos. Environ., 42, 6247-6260, https://doi.org/10.1016/j.atmosenv.2008.01.070, 2008.

Millet, D. B., Baasandorj, M., Hu, L., Mitroo, D., Turner, J., and Williams, B. J.: Nighttime Chemistry and Morning Isoprene Can Drive Urban Ozone Downwind of a Major Deciduous Forest, Environ. Sci. Technol., 50, 4335-4342, https://doi.org/10.1021/acs.est.5b06367, 2016.

Paatero, P.: User's Guide for positive Matrix Factorization programs PMF2 and PMF3, part 1-2: Tutorial, 19 -21. University of Helsinki, Helsinki, Finland, 2007.

Polissar, A. V., Hopke, P. K., Paatero, P., Malm, W. C., and Sisler, J. F.: Atmospheric aerosol over Alaska: 2. Elemental composition and sources, J. Geophys. Res.-Atmos., 103, 19045-19057, https://doi.org/10.1029/98jd01212, 1998.

US EPA: EPA Positive Matrix Factorization (PMF) 5.0 Fundamentals and User Guide, http://www.epa.gov/heasd/documents/ EPA. PMF.5.0.User.Guide. pdf, 2014.

Wang, H.-l., Jing, S.-a., Lou, S.-r., Hu, Q.-y., Li, L., Tao, S.-k., Huang, C., Qiao, L.-p., and Chen, C.-h.: Volatile organic compounds (VOCs) source profiles of on-road vehicle emissions in China, Sci. Total Environ., 607-608, 253-261, https://doi.org/10.1016/j.scitotenv.2017.07.001, 2017.

Wang, H., Qiao, Y., Chen, C., Lu, J., Qiao, L., and Lou, S.: Source Profiles and Chemical Reactivity of Volatile Organic Compounds from Solvent Use in Shanghai, China, Aerosol Air Qual. Res., 14, 301-310, https://doi.org/10.4209/aaqr.2013.03.0064, 2014.

Watson, J. G., Chow, J. C., and Fujita, E. M.: Review of volatile organic compound source apportionment by chemical mass balance, Atmos. Environ., 35, 1567-1584, 2001.

Yuan, B., Shao, M., Lu, S., and Wang, B.: Source profiles of volatile organic compounds associated with solvent use in Beijing, China, Atmos. Environ., 44, 1919-1926, https://doi.org/10.1016/j.atmosenv.2010.02.014, 2010.

Yuan, Z., Lau, A. K. H., Shao, M., Louie, P. K. K., Liu, S. C., and Zhu, T.: Source analysis of volatile organic compounds by positive matrix factorization in urban and rural environments in Beijing, J. Geophys. Res., 114, D00G15, https://doi.org/10.1029/2008jd011190, 2009.

Zhang, Y., Shao, M., Lin, Y., Luan, S., Mao, N., Chen, W., and Wang, M.: Emission inventory of carbonaceous pollutants from biomass burning in the Pearl River Delta Region, China, Atmos. Environ., 76, 189-199, https://doi.org/10.1016/j.atmosenv.2012.05.055, 2013.